Consequences of Neurite Transection *In Vitro*

Nurettin Cengiz,[1,2] Gürkan Öztürk,[3,4] Ender Erdoğan,[1,5] Aydın Him,[3,6] and Elif Kaval Oğuz[7]

Abstract

In order to quantify degenerative and regenerative changes and analyze the contribution of multiple factors to the outcome after neurite transection, we cultured adult mouse dorsal root ganglion neurons, and with a precise laser beam, we transected the nerve fibers they extended. Cell preparations were continuously visualized for 24 h with time-lapse microscopy. More distal cuts caused a more elongated field of degeneration, while thicker neurites degenerated faster than thinner ones. Transected neurites degenerated more if the uncut neurites of the same neuron simultaneously degenerated. If any of these uncut processes regenerated, the transected neurites underwent less degeneration. Regeneration of neurites was limited to distal cuts. Unipolar neurons had shorter regeneration than multipolar ones. Branching slowed the regenerative process, while simultaneous degeneration of uncut neurites increased it. Proximal lesions, small neuronal size, and extensive and rapid neurite degeneration were predictive of death of an injured neuron, which typically displayed necrotic rather than apoptotic form. In conclusion, this *in vitro* model proved useful in unmasking many new aspects and correlates of mechanically-induced neurite injury.

Key words: axonal injury; axonal regeneration; degeneration; neuronal cell death

Introduction

WHEN A PROCESS of a neuron is severed, several changes are initiated distal and proximal to the lesion site, as well as in the perikaryon. In vertebrates, the distal part of an injured neurite invariably degenerates in a fashion described by Augustus Waller more than 150 years ago.[1] The proximal part of the neurite may also degenerate, causing a somatopetal "dying-back" type of fiber loss that is thought to be linked to wallerian degeneration.[2–4]

Damaging nervous tissue in living animals is a common practice to study the mechanism of ensuing degenerative and regenerative processes. Sciatic and optic nerve transection, spinal cord transection, and cortical wounding, are among the major *in vivo* interventions utilized.[5–8] Such *in vivo* experiments have helped explain certain aspects of the neuronal response to neuritic injury, but have failed to answer some basic questions. For example, the proportions of apoptosis versus necrosis in the neuronal death seen following nerve injury are not fully known, primarily due to a lack of direct observation of the dying neurons.[9,10] Further, this also precludes the description of a potential correlation between vulnerability and size of an injured neuron, since dying neurons may atrophy or disappear completely. Despite a limited number of re-

ports,[11,12] the dying-back pattern of cut neurites has not been systematically examined.

There are several types of *in vitro* methods by which nervous tissue elements can be damaged in isolation in controlled culture conditions. Mechanical impactors;[13] micro-knives scissors, blades, and scalpels;[14–20] mechanical stretchers;[21] glass capillaries;[22] water-jets;[23] and weight drop;[24,25] are among the tools and techniques used for simulating neuronal injury *in vitro*. Though surgery with a laser beam is easier and more precise to apply, it has been employed in only a limited number of studies. A laser beam was first systematically utilized to cut neurites *in vitro* by Higgins and colleagues.[26–29] In these experiments, they cultured a mixed population of cells from embryonic mouse spinal cord. With a UV laser, they targeted dendrite-like extensions originating from the neurons on a cluttered carpet of non-neuronal cells.

In this study, we cultured isolated adult mouse dorsal root ganglion (DRG) neurons in high purity, and with a micro laser beam we made precise cuts of the extended neurites without damaging neighboring structures. Coupled with long-term time-lapse microscopy and extensive image analysis, we investigated the contributions of several injury-related and cellular parameters to the outcome of neuritic trauma.

[1]Department of Histology and Embryology, [3]Department of Physiology, Yüzüncü Yil University Medical School, Van, Turkey.
[2]Department of Histology and Embryology, Sakarya University Medical School, Sakarya, Turkey.
[4]Department of Physiology, Istanbul Medipol University, School of Medicine, Istanbul, Turkey.
[5]Department of Histology and Embryology, Selçuk University Medical School, Konya, Turkey.
[6]Department of Physiology, Ondokuz Mayis University Medical School, Samsun, Turkey.
[7]Department of Primary Education, Yüzüncü Yil University, Faculty of Education, Van, Turkey.

TABLE 1. VARIABLES IN THE PARAMETERS OF *IN VITRO* NEURITE TRANSECTION

Variable		Explanation
Polarity	Unipolar	
	Multipolar	
	No. of neurites	
Neurite thickness	Thin	Neurite diameter $<1\,\mu m$ at transection site
	Thick	Neurite diameter $>1\,\mu m$ at transection site
Neuronal surface area	μm^2	
Degeneration	Total length (μm)	
	Duration (min)	
	Rate ($\mu m/h$)	
Regeneration	Presence/absence	
	Starting time (min)	
	Length (μm)	
	Duration (min)	
	Rate ($\mu m/h$)	Computed data
	Bifurcation (presence absence)	Branching of neurites while regenerating
	Growth of uncut neurites (presence/absence)	Continuing growth of a neurite other than the one cut
Death	Presence/absence	Nuclear staining with propidium iodide
	Time (min)	Time until neuron dies
	Apoptotic/necrotic	Type of death according to visual criteria

Methods

Procedures involving animals and their care were conducted in conformity with institutional guidelines that are in compliance with EEC Council Directive 86/609. All efforts were made to minimize animal suffering and to minimize the number of animals used. Institutional ethical committee approval was obtained prior to the conduct of our experiments.

Cell culture

Young adult (6–8 weeks) BALB-C mice were anesthetized by an IP injection of ketamine (100 mg/kg; Pfizer, Istanbul, Turkey) and euthanized by cervical transection; 15–20 DRGs were quickly and aseptically removed under a stereomicroscope. After trimming all attached nerves in RPMI 1640 medium (Sigma-Aldrich, St. Louis, MO), they were transferred to Neurobasal A medium supplemented with 2% B27 (NBA-B27; Invitrogen, Carlsbad, CA) containing 2 mM Glutamax-I (Invitrogen), 100 U penicillin, 100 mg streptomycin, 250 ng/mL amphotericin B (Sigma-Aldrich), and 100 U/mL collagenase (Sigma-Aldrich). After 50 min of incubation in an incubator (37°C, 5% CO_2), the DRGs were washed in Hank's buffered salt solution (Sigma-Aldrich) three times, and subjected to further enzymatic digestion with trypsin (1 mg/mL) in NBA-B27 for 15 min in the incubator. The DRGs were then triturated for 15 min by gently and repeatedly pipetting through the tips of narrowing bores (from 2 mm diameter down), and finally through a 26-gauge injector needle. DNAse (50 μg/mL; Sigma-Aldrich) was added to the cell suspension obtained, which was then returned to the incubator and maintained there for another 30 min, this time on a custom-made agitator horizontally vibrating at 50 Hz. After this, the suspension was spun at 120g for 3 min, the supernatant was discarded, and the pellet was resuspended in NBA-B27 containing 10% fetal calf serum (Sigma-Aldrich) and 700 μg/mL trypsin inhibitor (Sigma-Aldrich) to neutralize the activity of the residual digestive enzymes. The cell suspension was then carefully pipetted on top of a three-layer Percoll (Sigma-Aldrich) gradient (60%, 35%, and 10% from bottom to top) prepared with NBA-B27 in a plastic tube and spun at 3000g for 20 min in a centrifuge cooled to 4°C. Neurons were collected from the 35% layer, washed with NBA-B27, and spun once more at 120g for 3 min; the supernatant was discarded and the pellet was resuspended in NBA-B27.

This final cell suspension was seeded on 35-mm glass-bottomed Petri dishes, which had been previously covered with poly-L lysine (1.8 μg/cm^2, 3 h at room temperature), and then laminin (40 ng/mm^2, overnight at 37°C). The dishes were left in the incubator for 2 h to let the neurons attach to the bottom, after which they were gently washed to remove unattached cells and remaining debris, and finally they were filled with NBA-B27 and returned to the incubator.

Laser microdissection

Within hours of incubation, DRG neurons began to give rise to regenerating neurites, which then became elongated enough to be transected 48 h later. To this end, appropriate neurons were selected on a computer-controlled inverted microscope with a stage incubator that creates a physiological atmosphere for the preparations (Cell Observer; Zeiss, Oberkochen, Germany); their coordinates

TABLE 2. RESULTS OF NEURITE TRANSECTION BASED ON THE DISTANCE OF TRANSECTION FROM THE PERIKARYON

No. of neurons		Distance of transection (μm)			Sham	Control	
		25 131	*150* 106	*300* 96	*94*	*132*	$p<0.05$
Degeneration	Length (μm)	22.9 ± 0.5	89.1 ± 28.6	152.6 ± 9.0			150 and 300 versus 25; 150 versus 300
	Rate ($\mu m/h$)	14.5 ± 0.9	42.6 ± 5.4	63.3 ± 12.2			150 and 300 versus 25; 150 versus 300
Regeneration		1 (0.8%)	13 (12.3%)	14 (14.6%)			150 and 300 versus 25
	Starting time (min)	120	218.5 ± 31.1	141.7 ± 14.8			150 versus 300 (25 not included in analysis because of small sample size)
	Length (μm)	27	49.1 ± 7.4	69.1 ± 9.0			
	Rate ($\mu m/h$)	4.5	15.2 ± 4.5	14.6 ± 2.1			
	Branching	1 (100%)	6 (46.2%)	7 (50%)			
Death	Rate	60 (45.8%)	19 (17.9%)	19 (19.8%)	0	10 (7.6%)	25, 150, and 300 versus sham and control; 150 and 300 versus 25
	Time (min)	229.1 ± 25.2	262.3 ± 80.9	408.3 ± 79.6		339 ± 47	25 versus 300
	Apoptotic	25 (19.1%)	5 (4.7%)	6 (6.3%)		5 (3.8%)	
	Necrotic	35 (26.7%)	14 (13.2%)	13 (13.5%)		5 (3.8%)	

TABLE 3. COMPARISON OF DEGENERATION LENGTH AND RATE BASED ON VARIOUS PARAMETERS

		Degeneration length (μm)/rate (μm/h)		
Distance of transection (μm) No. of neurons		25 131	150 106	300 96
Polarity	Unipolar	22.9±1/14.7±1.7 (37)	89.1±7.9/31.9±6.8 (38)	171.3±14.8/74.2±19.4 (29)
	Multipolar	22.9±0.6/14.4±1.1 (86)	89.1±5.7/49.1±7.6 (62)	144±11.3/58.3±15.5 (63)
Neurite thickness	Thin	20.9±3.2/15.5±4.5 (7)	71.4±25.1/44.1±24 (5)	63.3±36.5*/37.6±13.3 (4)
	Thick	23.1±0.5/14.4±0.9 (116)	90±4.7/42.5±5.6 (95)	156.7±9.2/64.5±12.7 (88)
Degeneration of uncut neurites	Present	23.4±0.6/15.3±1.2 (76)	97±5.1*/41.9±7.3 (62)	176.3±11.4/60.5±18.3 (53)
	Absent	22.1±1/13.2±1.4 (47)	76.2±8.3/43.7±8 (38)	120.4±13.3/67.1±14.6 (39)
Growth of uncut neurites	Present	20.6±2/14.8±3.3 (18)	48.3±11.7*/53.8±12.7 (16)	86.4±18.3*/44.6±9.2 (19)
	Absent	23.3±0.5/14.4±0.9 (106)	96.9±4.5/40.4±6 (84)	169.8±9.5/68.1±15.1 (73)

*$p < 0.05$.
Comparisons were made between two alternative forms or states of each parameter. Numbers of neurons are given in parentheses.

were recorded, and marks corresponding to the coordinates were placed on the lid of the dish to serve as a reference. During selection, any neurons exhibiting signs of stress, such as vacuoles, blebs, deformed membranes, or beaded neurites, were excluded. To further ensure the manipulation of only viable cells, propidium iodide (PI; Sigma-Aldrich) was added to the medium (7.5 μM), and the absence of nuclear staining in the selected neurons was confirmed. Before proceeding to the next stage, the neurites to be cut were marked on the electronic images taken, and the exact points of transection at 25, 150, or 300 μm from the perikaryon were marked on the printouts. For sham experiments, after the neuronal selection, an empty point 25 μm away from the perikaryon was marked in select preparations. Further controls were employed in which some neurons were selected but not cut.

Neurite transections of the selected neurons were performed on an inverted microscope (Zeiss Axiovert 200) equipped with a UV laser unit that operates at 337 nm and produces 1–30 pulses per second, each lasting 3 nsec and releasing approximately 300 μJ of energy. A 63× dry-phase contrast objective (LD Achroplan N.A. 0.75; Zeiss) was used during laser transections. The entire procedure was carried out using dedicated software, which has controls for the laser beam, microscope, and attached CCD camera. The laser was employed at an intensity of 65% and focal length of 21 (relative units) for approximately 1 sec for each transection. The transections were precise, disrupted no other part of the cell, and

created a clearly visible gap in the course of the targeted neurite. The sham injuries, which were focused on empty areas, received no neurite transection. During the laser microdissection, the cell preparations were left outside the incubator no longer than 30 min to avoid any substantial change in the pH of the culture medium.

Time-lapse microscopy

After the microdissection procedure, the preparations were transferred to a computer-controlled time-lapse microscopy system (Cell Observer; Zeiss), where multiple positions of a preparation could be imaged at desired time intervals over long periods, while a physiological environment (37°C and neutral pH maintained with heated air containing 5% CO_2) could be created for the cells with an integrated stage-top incubator (for a detailed description, see reference 30). To visualize the death of the neurons, PI was added to the culture medium. Phase contrast and fluorescence images of individual cells were digitally captured every 5 min for 24 h. The process was programmed and automatically executed using Axiovision 3.0 software.

Image and statistical analyses

Image analyses were performed with Axiovision 3.0, and included measurement, detection, and identification of several

TABLE 4. COMPARISON OF REGENERATION LENGTH AND RATE BASED ON VARIOUS PARAMETERS

		Regeneration length (μm)/rate (μm/h)	
Distance of transection (μm) No. of neurons		150 106	300 96
Polarity	Unipolar	42.4±14.1*/16.7±11.8 (5)	71.7±26.8/12.6±4 (3)
	Multipolar	53.3±8.8/14.3±2.7 (8)	68.4±9.7/15.1±2.6 (11)
Neurite thickness	Thin	67/5.5 (1)	115±10/23.6±12.4 (2)
	Thick	47.6±8/16.1±4.9 (12)	61.4±8.5/13.1±1.6 (12)
Bifurcation	Present	51.2±11.5/7.4±2.4* (6)	78.1±12.4/11±2 (7)
	Absent	47.3±10.5/22±7.5 (7)	60±13/18.2±3.5 (7)
Degeneration of uncut neurites	Present	46.8±12.8/29.7±8.6* (5)	60.6±18.3/14.1±2 (5)
	Absent	50.5±9.7/6.2±0.9 (8)	73.8±10.2/14.9±3.3 (9)
Growth of uncut neurites	Present	53.6±8.8/19.7±6 (9)	60.6±9.5/15.7±2.8 (10)
	Absent	39±14.5/5.2±1 (4)	90.3±18.3/11.8±2.6 (4)

*$p < 0.05$.
Comparisons were made between two alternative forms or states of each parameter. Numbers of neurons are given in parentheses. Since only one neurite regenerated in 25-μm cut group, the related data were omitted.

TABLE 5. COMPARISON OF PARAMETERS FOR NEURONS THAT SURVIVED NEURITE TRANSECTION WITH THOSE THAT DIED

Distance of transection (μm)		Live			Dead			
		25	150	300	25	150	300	$p < 0.05$
No. of neurons		71	87	77	60	19	19	
Polarity	Unipolar	19 (26.8%)	33 (37.9%)	24 (31.2%)	22 (36.7%)	7 (36.8%)	6 (31.6%)	
	Multipolar	52 (73.2%)	54 (62.1%)	53 (68.8%)	38 (63.3%)	12 (63.2%)	13 (68.4%)	
	No. of neurites	3±0.3	2.3±0.3	2.2±0.2	2.2±0.3	2.1±0.5	2.2±0.5	
Neurite thickness	Thin	3 (4.2%)	5 (5.8%)	4 (5.2%)	4 (6.7%)	0 (0%)	0 (0%)	
	Thick	68 (95.8%)	82 (94.2%)	73 (94.8%)	56 (93.3)	19 (100%)	19 (100%)	
Neuronal surface area (μm^2)		996.3±80.14	1219±85	1174±94.1	763.7±74.7	799.3±150	931.4±138.8	25, 150
Degeneration	Length (μm)	22.6±0.8	82.5±5	137.7±9.3	23.3±0.7	117.2±9	213.7±21.4	150, 300
	Rate (μm/h)	12.8±1.2	27.1±3.4	40.1±5.6	16.2±1.3	108.4±18.4	158.7±53.2	150, 300
	Degeneration of uncut neurites	46 (64.8%)	53 (60.9%)	40 (51.9%)	33 (55%)	10 (52.6%)	14 (73.6)	
Regeneration		1 (1.4%)	13 (14.9%)	13 (16.9%)	0 (0%)	0 (0%)	1 (5.3%)	
	Length (μm)	27	49.1±7.4	68.7±9.7			74	
	Rate (μm/h)	4.5	15.2±4.5	14.3±2.3			17.76	

variables (Table 1). The moment when the nucleus of a neuron started to emit red fluorescence (i.e., when it was stained with PI) was recorded as the time of death for each cell. Apoptotic and necrotic deaths were determined according to the following criteria. Swelling and neuronal rupture, occasionally accompanied by continually growing blebs and a lack of nuclear shrinkage suggested necrotic death. Shrinkage of the entire cell together with the nucleus, temporary blebbing, disintegration of the cellular membrane, or eventual swelling and bursting with the occasional formation of apoptotic bodies were considered signs of apoptotic death.[10,31–33]

For the statistical evaluations, the SPSS 13 software package was used. For the comparison of means, first the data series were analyzed with the Kolmogorov-Smirnov test to assess their distribution characteristics, according to which parametric or nonparametric tests were selected for further analyses. These were Student's *t*-test, Mann-Whitney *U* test, Kruskall-Wallis test, and one-way analysis of variance (ANOVA), followed by *post-hoc* LSD tests. Correlations between different variables were sought with Pearson's correlation analysis. Nominal data were analyzed with chi-square tests.

All differences or correlations stated below imply statistical significance ($p < 0.05$), unless otherwise stated. Data were given as mean±standard error of the mean (SEM).

When the 150-μm and 300-μm cut groups had similar statistical properties, analyses were performed with the data pooled from both groups, and this was indicated by ''150+300.''

Results

Main quantitative findings regarding degeneration, regeneration, and survival, are summarized in Tables 2–5.

Description of events following neurite transection

Immediately following transection with the laser beam, both proximal and distal segments suddenly retracted due to passive recoil (Fig. 1; see Supplementary Video S1; see online supplementary material at http://www.liebertonline.com). This retraction typically involved a displacement of a few to tens of micrometers. This displacement appeared to depend on the structure of the cut neurite. Thick and flat neurites with filopodial extensions were attached more firmly to the substrate, and thus exhibited little or no

recoil. In contrast, thinner or occasionally stretched neurites had a stronger recoil. Sometimes the latter even caused the neurites to completely detach from the substrate, and such extreme samples were excluded from the analyses.

Most neurites started to degenerate immediately after transection, a process that continued for several hours. Some neurites regenerated after they were cut (Fig. 2 and Supplementary Video S2; see online supplementary material at http://www.liebertonline.com).

Degeneration

The amount, duration, and rate of degeneration following neurite transection were strongly correlated with the distance of transection from the perikaryon (Table 2). Although the length of degeneration varied between the 150-μm and 300-μm groups, its duration was similar.

Compared to thick neurites, the thinner neurites degenerated less (67.8±20 versus 122.1±5.6 μm for 150+300; Table 3). Further,
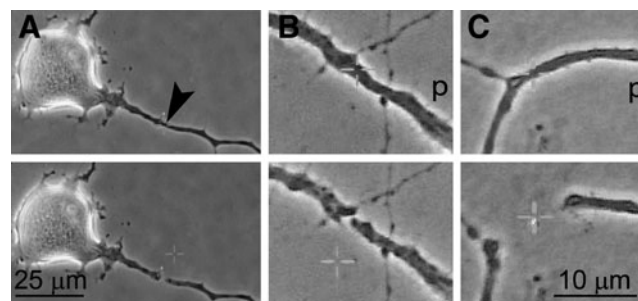

FIG. 1. Transection of a neurite with a laser beam and passive recoil of the cut ends. Cultured adult mouse primary sensory neurons grow neurites that are long enough by day 2 to be cut with a laser beam focused and activated for about 1 sec (A). The cut ends suddenly retract and are separated by a few (B) to tens of micrometers (C), depending on various factors (arrowhead indicates site of transection; p, proximal part of the neurite; see Supplementary Video S1; see online supplementary material at http://www.liebertonline.com).
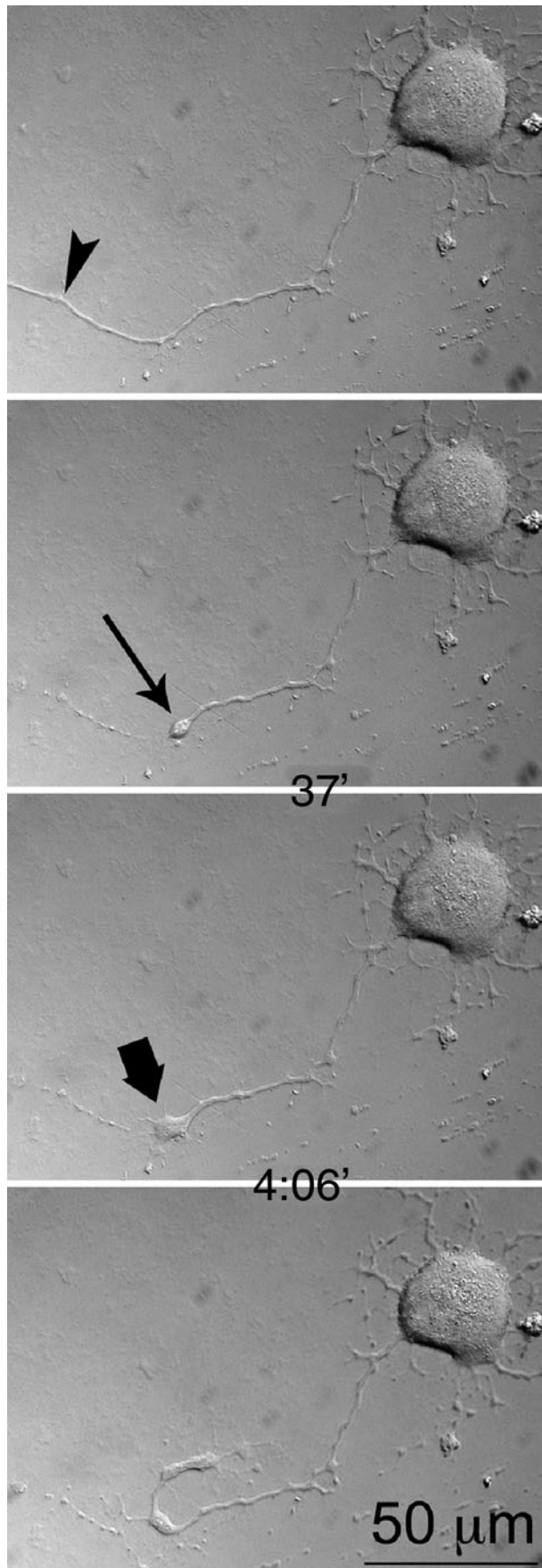
the length of degeneration was greater in a cut neurite when other extensions of the same cell simultaneously degenerated (98.6 ± 8 versus $133.5 \pm 7 \mu m$ for $150 + 300$), and shorter when they kept growing (129.6 ± 6 versus $69 \pm 12 \mu m$ for $150 + 300$).

Regeneration

More neurons regenerated their transected neurites when the transections were made at 150-μm or 300-μm distances versus those transected at $25 \mu m$ (Table 2). Regenerated neurons were larger (1101.9 ± 58.6 versus $1362.2 \pm 166.5 \mu m^2$ for $150 + 300$; Fig. 3).

Thinner neurites regenerated over longer distances (99 ± 17 versus $53 \pm 6 \mu m$ for $150 + 300$), while the neurites of multipolar neurons regenerated over longer distances than those of unipolar neurons after transection at $150 \mu m$ (Table 4). In neurons with regenerating transected neurites, the persisting neurites were more likely to continue growing (growth of uncut neurites 65.5% versus 11.1% with and without regeneration of transected neurites, respectively, for $150 + 300$). When uncut neurites underwent primary degeneration, the transected neurite of the same neuron manifested an accelerated regenerative rate after transection at $150 \mu m$ (Table 4). Another factor influencing the rate of regeneration was linked to the occurrence of branching, which slowed the regenerative process (20 ± 4 versus $9.3 \pm 1.5 \mu m/h$; $150 + 300$). There was no correlation between the number of total extensions per neuron and the tendency of a regenerating neurite to bifurcate.

Neuron survival

Significantly higher proportions of neurons died in the transected groups compared to sham and control cells (Table 2). In the 25-mm group, neurons were more likely to die than those that those transected at more remote sites, and they died earlier than those in the 300-μm group (Fig. 4, Table 2, and Supplementary Video S3; see online supplementary material at http://www.liebertonline .com).

Smaller neurons died in greater numbers and earlier than larger ones after injury (mean surface area $\pm$ SEM of neurons that died and survived the injury: 1198 ± 63 and $865 \pm 101 \mu m^2$, respectively; r = 0.4 for the correlation between time of death and mean surface area for $150 + 300$; Figs. 3 and 5, Table 5, and Supplementary Video S4; see online supplementary material at http://www.liebertonline .com). Following transection, regeneration of a cut neurite was a positive predictor for the likelihood of neuronal survival (death rate 3.45% versus 21.64% in the presence or absence of regeneration in a cut neurite, respectively, for $150 + 300$; Fig. 4 and Table 5). Even when the cut neurite failed to regenerate, the neuron was less likely to die if its other extensions continued to grow (death rate 0.5% versus 24% for $150 + 300$, in cells with continuing growth or not, respectively). In contrast, the neurons that did not survive transection were those that displayed degeneration over longer lengths (164.1 ± 13.8 versus $108.9 \pm 5.6 \mu m$ in dying and surviving neurons, respectively, for $150 + 300$). Neurons were more likely to die and to die earlier as the rate of degeneration increased (132.8 ± 27.5 versus

FIG. 2. Regeneration of a transected neurite (arrowhead indicates site of laser transection). A growth cone (bold arrow) is formed from a retraction bulb (arrow). Note that the first image shows the intact neurite before transection, and that the time intervals at which the images were taken are shown between frames (see Supplementary Video S2; see online supplementary material at http://www.liebertonline.com).
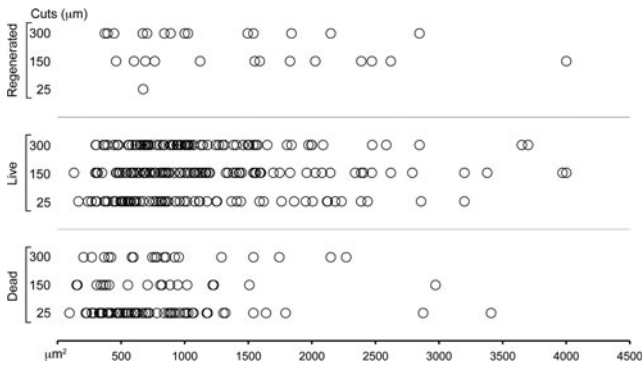
FIG. 3. Size distribution of primary sensory neurons that survived, died, or regenerated within 24 h after neurite transection at three different distances from the cell body.

$33.3 \pm 3.3 \, \mu m/h$ in dying and surviving neurons, respectively; $r = -0.44$ for the correlation between time of death and degeneration rate for $150 + 300$).

Although more neurons appeared to die necrotically than apoptotically, no significant difference or correlation was demonstrated among groups based on any independent variable, with the exception of time of death. Necrotic death occurred more rapidly than apoptotic death (246.3 ± 51.9 versus 541.5 ± 130.4 min; Fig. 6 and Supplementary Videos S5a and S5b; see online supplementary material at http://www.liebertonline.com). Another factor accelerating death was smaller neuronal size ($r = 0.391$).

Discussion

Neurite outgrowth in cultured neurons

The size and polarity of the neurons in culture had variations. Small and large neurons were found in almost equal proportions, with both unipolar (30%) and multipolar (70%) profiles (data not shown). Such phenotypic variations among DRG neurons have been reported by others.[34–36] Neurons initiated neurite extension within hours of incubation. In separate sets of experiments we performed immunohistochemical staining for the major cytoskeletal proteins (neurofilaments, tubulin, and actin), and found that even newly-growing neurites contain these proteins (data not shown). Thus their content is comparable to that found *in vivo*.

The extent of degeneration depends on the site of lesion and axonal diameter

Neurites degenerated more when the cut was made farther from the body, and degeneration occurred more rapidly. Neuritic degeneration following transection involves activation of proteolytic enzymes such as calpains, which are activated by increased intracellular calcium with subsequent degradation of cytoskeletal
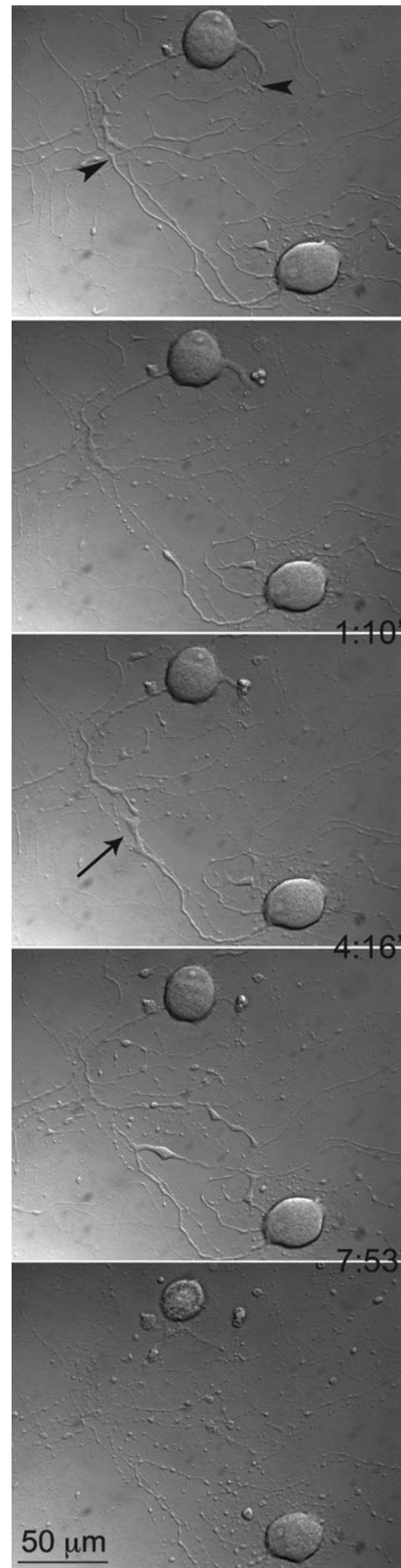
FIG. 4. The effect of the distance of neurite transection from the soma on the survival of the neurons. A close neurite transection caused the upper neuron to die, while the lower neuron, with more distant transection, was still alive and regenerated the cut neurite (arrow). Note that the first image demonstrates the intact neurite before transection, and that the time intervals at which the images were taken are shown between frames. Arrowheads indicate the sites of laser transection. (See Supplementary Video S3; see online supplementary material at http://www.liebertonline.com.)
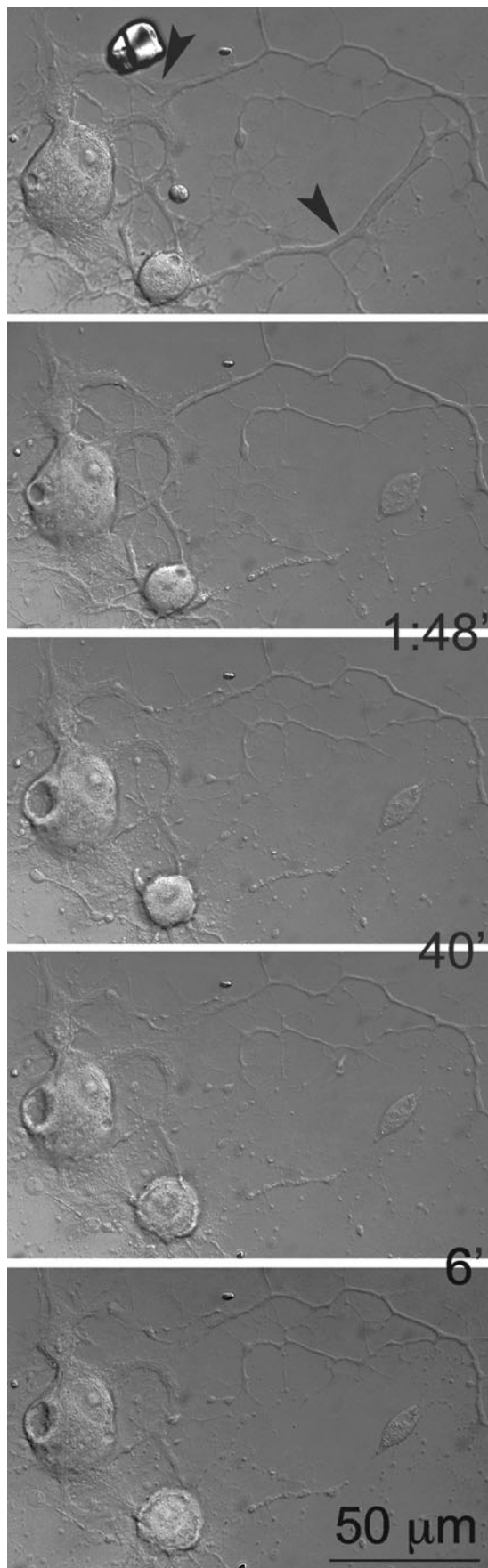
proteins. This process also elicits vesicle formation that helps form an effective seal of the transected neurite.[37] Neurofilament proteins have a lower density in the distal part of a nerve fiber than its more proximal segments.[38] It is thought that the higher protein content in the proximal segment makes resealing more likely than in the distal portion. This may also relate to our finding that more remote transection resulted in longer lengths of degeneration.

We observed shorter distances of degeneration in thin neurites, which may be explained by the more rapid resealing of the cut ends and a reduced influx of Ca^{++}.[39] This finding is consistent with reports indicating that small fibers are less affected by injury,[40,41] but is contrary to other reports suggesting the opposite,[42–45] or suggesting no size preference.[46]

Multiple factors determine the fate of injured neurons

It has been reported that transection of a neurite close to the soma is associated with a higher risk of neuronal cell death than that seen with more remote lesions in motoneurons,[47,48] rubrospinal neurons,[49,50] spinal neurons,[29] neuroblastoma cells,[39] spinocerebellar neurons of Clarke's column,[51] and olfactory neurons.[52] However, following traumatic brain injury, axotomy within 25–50 μm of the soma has been reported not to cause neuronal death, most likely due to the different pathogenesis of axotomy versus direct neurite transection.[53] We found a significantly higher rate of cell death following transection at 25 μm than that seen with more distal transection; however, the rate of cell death was no different between transections at 150 and 300 μm. Our 19% death rate in the latter is comparable to that reported by others (18%[54] and 20–25%),[55] which were obtained in *in vivo* experiments. This finding may suggest contributions of different mechanisms to the survival of neurons following ultra-close or distant neurotomies. Indeed, different explanations have been postulated for the survival of neurons that differ according to proximity of the injury to the cell body. Some suggest that a distal neurotomy means more spared collaterals, and thus an uninterrupted supply of target-derived trophic factors.[56] A more plausible explanation for our observation is that ultra-close lesions permit the influx of concentrations of extracellular Ca^{++},[39] generating a stronger injury current[29,57] to reach the cell body, and thereby cause more destruction.

Smaller neurons, which are probably involved in nociception,[58] were most susceptible to death and they died earlier. Previous *in vivo* studies suggested a similar relationship between the size of primary sensory neurons and their vulnerability to neurotomy-induced changes.[59–62] However, since axotomized neurons undergo atrophy whether they ultimately die or survive, it was not possible to identify if any atrophic cell observed once belonged to the large-diameter neuron population. This study is the first direct quantification of this phenomenon. The reason for the greater susceptibility of smaller neurons might be related to their loss of internal homeostasis. Another potential mechanism may be related to small sensory neuron interactions with nerve growth factor

FIG. 5. The effect of cell size on the survival of neurons after neurite transection. The small neuron dies while the larger one was still alive. Note that the first image demonstrates the intact neurite before transection, and that the time intervals at which the images were taken are shown between frames. Arrowheads indicate sites of laser transection. (See Supplementary Video S4; see online supplementary material at http://www.liebertonline.com.)
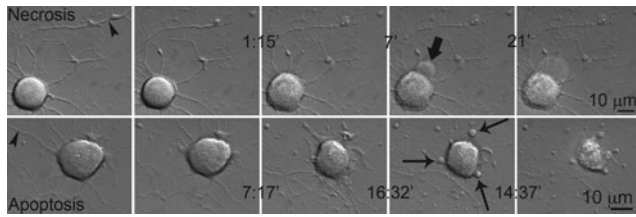
FIG. 6. Death by apoptosis and necrosis after neurite transection. Necrotic death occurs earlier than apoptotic death. The bold arrow indicates a growing bleb that has burst in the next frame. Thin arrows indicate apoptotic bodies being formed. Note that the first images in both rows demonstrate intact neurites before transection, and that the time intervals at which the images were taken are shown between frames. Arrowheads indicate sites of laser transection. (See Supplementary Videos S5a and S5b; see online supplementary material at http://www.liebertonline.com.)

(NGF). Normally, these cells express high-affinity TrkA receptors for this factor,[36] with NGF acting at the end of a neurite not only to save the neurite from degeneration, but also to trigger cell body signalling to blunt the onset of apoptosis, even if the cell body itself was not exposed to this factor.[63] We do not add growth factors to our cultures, which may alter small-cell vulnerability to injury-induced changes. Since a cell may completely disappear after dying, it is impossible to know in *in vivo* studies whether apoptotic profiles are the only cells lost. Necrosis develops very quickly, which makes it very difficult to detect. Due to such technical problems, the actual rates of neuronal necrosis and apoptosis after peripheral damage have not been elucidated. In this study, injured neurons mostly died necrotically, which occurred significantly earlier than apoptosis. However, we found no correlation between the variables examined in this study and the likelihood of a neuron to die via apoptosis or necrosis. Longer as well as more rapid degeneration was associated with a higher rate of death.

We suggest that an injured neuron in poor overall condition is susceptible to more extensive degeneration, probably due to a lack of resources for successful resealing, or to maintain cellular integrity. Extensive neurite degeneration also makes the neuron's health even poorer.

Although thinner neurites had less degeneration, this did not translate into better neuronal survival. This might be because thin neurites most likely belonged to the death-prone, smaller neuron population.

Regeneration of neurites after transection

The number of studies that have examined regeneration of neurites after *in vitro* transection is limited.

Spinal neurons did not regrow their neurites after laser axotomy.[29] However, regeneration started within 2 h after transection in embryonic cortical[15] and sympathetic[23,64] neuron cultures and embryonic chick DRG explants.[22] While we observed only one incidence of regeneration after transection at 25 μm, 12.3% and 14.6% of all neurites re-grew after they were cut at 150 and 300 μm, respectively. Ultra-close injuries are associated with a higher rate of death and greater disturbance of intracellular homeostasis, which may explain the nearly non-existent regeneration. An additional factor may be the degeneration of the complete proximal stump in most cases, which could otherwise be used as a kernel upon which cellular reconstruction could occur. Indeed, it has been demon- strated that newly-regenerating axons use existing cytoskeletal elements in the proximal stump.[65] Consistent with this, we found that the earliest onset of regeneration was seen with longer proximal stumps (after transection at 300 μm).

An important factor determining the total distance and rate of regeneration is the supply of material for new construction.[66] Larger neurons re-grew cut neurites more often than smaller ones, which might be related to a more abundant supply of this material. The more extensive regeneration of multipolar neurons might also be related to translocation of cytoskeletal elements from other extensions into the growing neurite. The presence of other processes did not increase the length or rate of re-growth after transection at 300 μm. This was probably due to the already high capacity of the longer proximal stump to act as a resource for structural elements.[65] Bifurcation during growth slowed neurite regeneration, probably due to the lag caused by complex reorganization of the cytoskeleton. The polarity of a neuron was not predictive of whether a growing neurite would branch or not. Thus a phenotypic predetermination did not exist.

Author Disclosure Statement

No competing financial interests exist.

References

1. Waller, A. (1850). Experiments on the section of the glossopharyngeal and hypoglossal nerves of the frog, and observations of the alterations produced thereby in the structure of their primitive fibres. Philos. Trans. R. Soc. Lond. B. Biol. Sci. 140, 423–429.
2. Bouldin, T.W., and Cavanagh, J.B. (1979). Organophosphorus neuropathy. I. A teased-fiber study of the spatio-temporal spread of axonal degeneration. Am. J. Pathol. 94, 241–252.
3. Cavanagh, J.B. (1979). The 'dying back' process. A common denominator in many naturally occurring and toxic neuropathies. Arch. Pathol. Lab. Med. 103, 659–664.
4. Samsam, M., Mi, W., Wessig, C., Zielasek, J., Toyka, K.V., Coleman, M.P., and Martini, R. (2003). The Wlds mutation delays robust loss of motor and sensory axons in a genetic model for myelin-related axonopathy. J. Neurosci. 23, 2833–2839.
5. Fry, E.J., Ho, C., and David, S. (2007). A role for Nogo receptor in macrophage clearance from injured peripheral nerve. Neuron 53, 649–662.
6. Hu, Y., Cui, Q., and Harvey, A.R. (2007). Interactive effects of C3, cyclic AMP and ciliary neurotrophic factor on adult retinal ganglion cell survival and axonal regeneration. Mol. Cell. Neurosci. 34, 88–98.
7. Petruska, J.C., Ichiyama, R.M., Jindrich, D.L., Crown, E.D., Tansey, K.E., Roy, R.R., Edgerton, V.R., and Mendell, L.M. (2007). Changes in motoneuron properties and synaptic inputs related to step training after spinal cord transection in rats. J. Neurosci. 27, 4460–4471.
8. Taylor, A.N., Rahman, S.U., Tio, D.L., Sanders, M.J., Bando, J.K., Truong, A.H., and Prolo, P. (2006). Lasting neuroendocrine-immune effects of traumatic brain injury in rats. J. Neurotrauma 23, 1802–1813.
9. Berkelaar, M., Clarke, D.B., Wang, Y.C., Bray, G.M., and Aguayo, A.J. (1994). Axotomy results in delayed death and apoptosis of retinal ganglion cells in adult rats. J. Neurosci. 14, 4368–4374.
10. Groves, M.J., Christopherson, T., Giometto, B., and Scaravilli, F. (1997). Axotomy-induced apoptosis in adult rat primary sensory neurons. J. Neurocytol. 26, 615–624.
11. Houle, J.D., and Jin, Y. (2001). Chronically injured supraspinal neurons exhibit only modest axonal dieback in response to a cervical hemisection lesion. Exp. Neurol. 169, 208–217.

12. Oudega, M., Vargas, C.G., Weber, A.B., Kleitman, N., and Bunge, M.B. (1999). Long-term effects of methylprednisolone following transection of adult rat spinal cord. Eur. J. Neurosci. 11, 2453–2464.

13. Chu, G.K., and Tator, C.H. (2001). Calcium influx is necessary for optimal regrowth of transected neurites of rat sympathetic ganglion neurons in vitro. Neuroscience 102, 945–957.

14. Blizzard, C.A., Haas, M.A., Vickers, J.C., and Dickson, T.C. (2007). Cellular dynamics underlying regeneration of damaged axons differs from initial axon development. Eur. J. Neurosci. 26, 1100–1108.

15. Chuckowree, J.A., and Vickers, J.C. (2003). Cytoskeletal and morphological alterations underlying axonal sprouting after localized transection of cortical neuron axons in vitro. J. Neurosci. 23, 3715–3725.

16. Dickson, T.C., Adlard, P.A., and Vickers, J.C. (2000). Sequence of cellular changes following localized axotomy to cortical neurons in glia-free culture. J. Neurotrauma 17, 1095–1103.

17. Eddleman, C.S., Ballinger, M.L., Smyers, M.E., Godell, C.M., Fishman, H.M., and Bittner, G.D. (1997). Repair of plasmalemmal lesions by vesicles. Proc. Natl. Acad. Sci. USA 94, 4745–4750.

18. Schlaepfer, W.W., and Bunge, R.P. (1973). Effects of calcium ion concentration on the degeneration of amputated axons in tissue culture. J. Cell Biol. 59, 456–470.

19. Sievers, C., Platt, N., Perry, V.H., Coleman, M.P., and Conforti, L. (2003). Neurites undergoing Wallerian degeneration show an apoptotic-like process with Annexin V positive staining and loss of mitochondrial membrane potential. Neurosci. Res. 46, 161–169.

20. Yawo, H., and Kuno, M. (1983). How a nerve fiber repairs its cut end: involvement of phospholipase A2. Science 222, 1351–1353.

21. Geddes, D.M., LaPlaca, M.C., and Cargill, R.S., II (2003). Susceptibility of hippocampal neurons to mechanically induced injury. Exp. Neurol. 184, 420–427.

22. Gallo, G. (2004). Myosin II activity is required for severing-induced axon retraction in vitro. Exp. Neurol. 189, 112–121.

23. Campenot, R.B. (1982). Development of sympathetic neurons in compartmentalized cultures. I. Local control of neurite growth by nerve growth factor. Dev. Biol. 93, 1–12.

24. Balentine, J.D., Greene, W.B., and Bornstein, M. (1988). In vitro spinal cord trauma. Lab. Invest. 58, 93–99.

25. Wallis, R.A., and Panizzon, K.L. (1995). Felbamate neuroprotection against CA1 traumatic neuronal injury. Eur. J. Pharmacol. 294, 475–482.

26. Gross, G.W., Lucas, J.H., and Higgins, M.L. (1983). Laser microbeam surgery: ultrastructural changes associated with neurite transection in culture. J. Neurosci. 3, 1979–1993.

27. Higgins, M.L., Smith, M.N., and Gross, G.W. (1980). Selective cell destruction and precise neurite transection in neuroblastoma cultures with pulsed ultraviolet laser microbeam irradiation: an analysis of mechanisms and transection reliability with light and scanning electron microscopy. J. Neurosci. Methods 3, 83–99.

28. Kirkpatrick, J.B., Higgins, M.L., Lucas, J.H., and Gross, G.W. (1985). In vitro simulation of neural trauma by laser. J. Neuropathol. Exp. Neurol. 44, 268–284.

29. Lucas, J.H., Gross, G.W., Emery, D.G., and Gardner, C.R. (1985). Neuronal survival or death after dendrite transection close to the perikaryon: correlation with electrophysiologic, morphologic, and ultrastructural changes. Cent. Nerv. Syst. Trauma 2, 231–255.

30. Ozturk, G., and Erdogan, E. (2004). Multidimensional long-term time-lapse microscopy of in vitro peripheral nerve regeneration. Microsc. Res. Tech. 64, 228–242.

31. Barros, L.F., Stutzin, A., Calixto, A., Catalan, M., Castro, J., Hetz, C., and Hermosilla, T. (2001). Nonselective cation channels as effectors of free radical-induced rat liver cell necrosis. Hepatology 33, 114–122.

32. Barros, L.F., Kanaseki, T., Sabirov, R., Morishima, S., Castro, J., Bittner, C.X., Maeno, E., Ando-Akatsuka, Y., and Okada, Y. (2003). Apoptotic and necrotic blebs in epithelial cells display similar neck diameters but different kinase dependency. Cell Death Differ. 10, 687–697.

33. Majno, G., and Joris, I. (1995). Apoptosis, oncosis, and necrosis. An overview of cell death. Am. J. Pathol. 146, 3–15.

34. Delree, P., Ribbens, C., Martin, D., Rogister, B., Lefebvre, P.P., Rigo, J.M., Leprince, P., Schoenen, J., and Moonen, G. (1993). Plasticity of developing and adult dorsal root ganglion neurons as revealed in vitro. Brain Res. Bull. 30, 231–237.

35. Fukuda, J. (1985). Nerve cells of adult and aged mice grown in a monolayer culture: age-associated changes in morphological and physiological properties of dorsal root ganglion cells in vitro. Dev. Neurosci. 7, 374–394.

36. McMahon, S.B., Armanini, M.P., Ling, L.H., and Phillips, H.S. (1994). Expression and coexpression of Trk receptors in subpopulations of adult primary sensory neurons projecting to identified peripheral targets. Neuron 12, 1161–1171.

37. Xie, X.Y., and Barrett, J.N. (1991). Membrane resealing in cultured rat septal neurons after neurite transection: evidence for enhancement by Ca(2+)-triggered protease activity and cytoskeletal disassembly. J. Neurosci. 11, 3257–3267.

38. Schlaepfer, W.W., and Bruce, J. (1990). Neurofilament proteins are distributed in a diminishing proximodistal gradient along rat sciatic nerve. J. Neurochem. 55, 453–460.

39. Yoo, S., Bottenstein, J.E., Bittner, G.D., and Fishman, H.M. (2004). Survival of mammalian B104 cells following neurite transection at different locations depends on somal Ca2+ concentration. J. Neurobiol. 60, 137–153.

40. Donat, J.R., and Wisniewski, H.M. (1973). The spatio-temporal pattern of Wallerian degeneration in mammalian peripheral nerves. Brain Res. 53, 41–53.

41. Veronesi, B., and Boyes, W.K. (1988). Morphometric and electrophysiological evidence for a diameter-based rate of degeneration in the optic nerve of the rat. Exp. Neurol. 101, 176–189.

42. Friede, R.L., and Martinez, A.J. (1970). Analysis of axon-sheath relations during early Wallerian degeneration. Brain Res. 19, 199–212.

43. LoPachin, R.M., Jr., and Saubermann, A.J. (1990). Disruption of cellular elements and water in neurotoxicity: studies using electron probe x-ray microanalysis. Toxicol. Appl. Pharmacol. 106, 355–374.

44. Lubinska, L. (1977). Early course of Wallerian degeneration in myelinated fibres of the rat phrenic nerve. Brain Res. 130, 47–63.

45. Sugioka, M., Sawai, H., Adachi, E., and Fukuda, Y. (1995). Changes of compound action potentials in retrograde axonal degeneration of rat optic nerve. Exp. Neurol. 132, 262–270.

46. Malbouisson, A.M., Ghabriel, M.N., and Allt, G. (1985). Axonal degeneration in large and small nerve fibres. An electron-microscopic and morphometric study. J. Neurol. Sci. 67, 307–318.

47. Aldskogius, H., Barron, K.D., and Regal, R. (1980). Axon reaction in dorsal motor vagal and hypoglossal neurons of the adult rat. Light microscopy and RNA-cytochemistry. J. Comp. Neurol. 193, 165–177.

48. Mattsson, P., Meijer, B., and Svensson, M. (1999). Extensive neuronal cell death following intracranial transection of the facial nerve in the adult rat. Brain Res. Bull. 49, 333–341.

49. Giehl, K.M., and Tetzlaff, W. (1996). BDNF and NT-3, but not NGF, prevent axotomy-induced death of rat corticospinal neurons in vivo. Eur. J. Neurosci. 8, 1167–1175.

50. Tetzlaff, W., Kobayashi, N.R., Giehl, K.M., Tsui, B.J., Cassar, S.L., and Bedard, A.M. (1994). Response of rubrospinal and corticospinal neurons to injury and neurotrophins. Prog. Brain Res. 103, 271–286.

51. Loewy, A.D., and Schader, R.E. (1977). A quantitative study of retrograde neuronal changes in Clarke's column. J. Comp. Neurol. 171, 65–81.

52. Cancalon, P.F. (1987). Survival and subsequent regeneration of olfactory neurons after a distal axonal lesion. J. Neurocytol. 16, 829–841.

53. Singleton, R.H., Zhu, J., Stone, J.R., and Povlishock, J.T. (2002). Traumatically induced axotomy adjacent to the soma does not result in acute neuronal death. J. Neurosci. 22, 791–802.

54. Rich, K.M., Disch, S.P., and Eichler, M.E. (1989). The influence of regeneration and nerve growth factor on the neuronal cell body reaction to injury. J. Neurocytol. 18, 569–576.

55. Himes, B.T., and Tessler, A. (1989). Death of some dorsal root ganglion neurons and plasticity of others following sciatic nerve section in adult and neonatal rats. J. Comp. Neurol. 284, 215–230.

56. Bernstein-Goral, H., and Bregman, B.S. (1997). Axotomized rubrospinal neurons rescued by fetal spinal cord transplants maintain axon collaterals to rostral CNS targets. Exp. Neurol. 148, 13–25.

57. Borgens, R.B., Jaffe, L.F., and Cohen, M.J. (1980). Large and persistent electrical currents enter the transected lamprey spinal cord. Proc. Natl. Acad. Sci. USA 77, 1209–1213.

58. Vyklicky, L., and Knotkova-Urbancova, H. (1996). Can sensory neurones in culture serve as a model of nociception? Physiol. Res. 45, 1–9.

59. Groves, M.J., Ng, Y.W., Ciardi, A., and Scaravilli, F. (1996). Sciatic nerve injury in the adult rat: comparison of effects on oligosaccharide, CGRP and GAP43 immunoreactivity in primary afferents following two types of trauma. J. Neurocytol. 25, 219–231.

60. Guseva, D., and Chelyshev, Y. (2006). The plasticity of the DRG neurons belonging to different subpopulations after dorsal rhizotomy. Cell. Mol. Neurobiol. 26, 1225–1234.

61. Rich, K.M. (1992). Neuronal death after trophic factor deprivation. J. Neurotrauma 9, Suppl. 1, 61–69.

62. White, F.A., Bennett-Clarke, C.A., Macdonald, G.J., Enfiejian, H.L., Chiaia, N.L., and Rhoades, R.W. (1990). Neonatal infraorbital nerve transection in the rat: comparison of effects on substance P immunoreactive primary afferents and those recognized by the lectin *Bandeiraea simplicifolia*-I. J. Comp. Neurol. 300, 249–262.

63. Campenot, R.B. (1994). NGF and the local control of nerve terminal growth. J. Neurobiol. 25, 599–611.

64. Fayaz, I., and Tator, C.H. (2000). Modeling axonal injury in vitro: injury and regeneration following acute neuritic trauma. J. Neurosci. Methods 102, 69–79.

65. McQuarrie, I.G., and Lasek, R.J. (1989). Transport of cytoskeletal elements from parent axons into regenerating daughter axons. J. Neurosci. 9, 436–446.

66. McQuarrie, I.G. (1986). Structural protein transport in elongating motor axons after sciatic nerve crush. Effect of a conditioning lesion. Neurochem. Pathol. 5, 153–164.

Address correspondence to:
Gürkan Öztürk, M.D., Ph.D.
Istanbul Medipol Üniversitesi
Atatürk Bulv. No: 27
Istanbul, Fatih, 34083, Turkey

E-mail: gozturk@medipol.edu.tr